Calculation of predictions for non-identical particle correlations in AA collisions at LHC energies from hydrodynamics-inspired models

MASTER OF SCIENCE THESIS

Author:
Mateusz Wojciech Gałażyn

Supervisor:
Prof. Adam Kisiel

Warsaw, 29th July 2014

Obliczenia teoretycznych przewidywań korelacji cząstek nieidentycznych w zderzeniach AA przy energiach LHC pochodzących z modeli hydrodynamicznych

PRACA MAGISTERSKA

Autor:
Mateusz Wojciech Gałażyn

Promotor:
dr hab. inż. Adam Kisiel, prof. PW

Warszawa, 29 lipca 2014

Abstract

Streszczenie

Contents

Introduction

Chapter 1

Theory of heavy ion collisions

1.1 The Standard Model

In the 1970s, a new theory of fundamental particles and their interaction emerged. A new concept, which concerns the electromagnetic, weak and strong nuclear interactions between know particles. This theory is called *The Standard Model*. There are seventeen named particles in the standard model, organized into the chart shown below (Fig. 1.1). Fundamental particles are divided into two families: *fermions* and *bosons*.

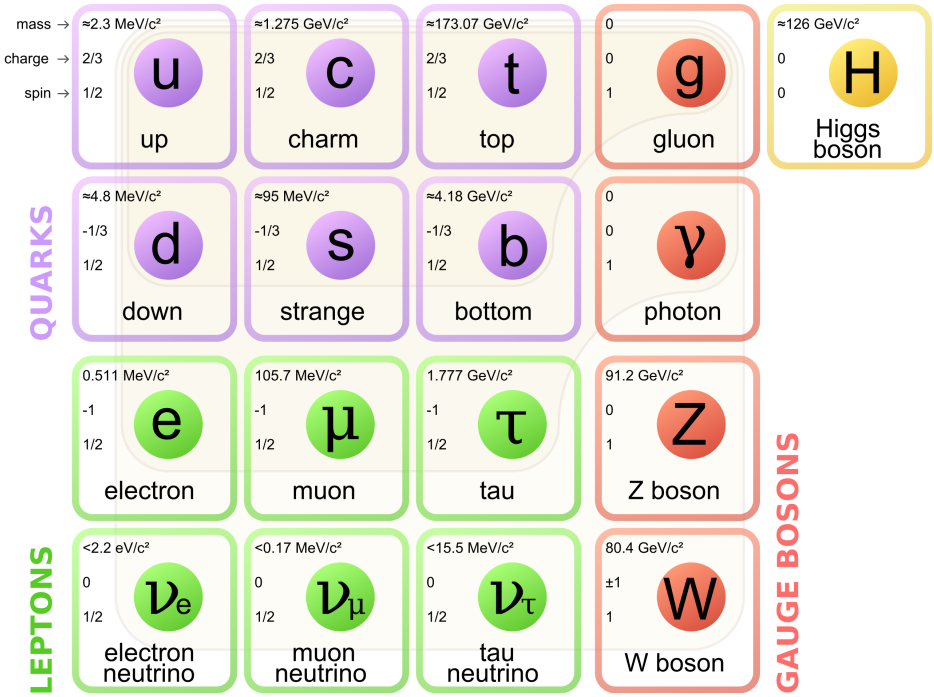

Figure 1.1: The Standard Model of elementary particles [1].

Fermions are the building blocks of matter. They are divided into two groups. Six of them, which must bind together are called *quarks*. Quarks are known to bind into doublets (*mesons*), triplets (*baryons*) and recently confirmed four-quark states.[1] Two of baryons, with the longest lifetimes, are forming a nucleus: a proton and a neutron. A proton is build from two up quarks and one down, and neutron consists of two down quarks and one up. A proton is found to be a stable particle (at least it has a lifetime larger than 10^{35} years) and a free neutron has a mean lifetime about 8.8×10^2 s. Fermions, that can exist independently are called *leptons*. Neutrinos are a subgroup of leptons, which are only influenced by weak interaction. Fermions can be divided into three generations (three columns in the Figure 1.1). Generation I particles can combine into hadrons with the longest life spans. Generation II and III consists of unstable particles which form also unstable hadrons.

Bosons are force carriers. There are four fundamental forces: weak - responsible for radioactive decay, strong - coupling quarks into hadrons, electromagnetic - between charged particles and gravity - the weakest, which causes the attraction between particles with a mass. The Standard Model describes the first three. The weak force is mediated by $W^{\pm}$ and Z^0 bosons, electromagnetic force is carried by photons γ and the carriers of a strong interaction are gluons g. The fifth boson is a Higgs boson which is responsible for giving other particles mass.

1.2 Quantum Chromodynamics

1.2.1 Quarks and gluons

Quarks interact with each other through the strong interaction. The mediator of this force is a *gluon* - a massless and chargeless particle. In the quantum chromodynamics (QCD) - theory describing strong interaction - there are six types of "charges" (like electrical charges in the electrodynamics) called *colours*. The colors were introduced because some of the observed particles, like Δ^-, Δ^{++} and Ω^- appeared to consist of three quarks with the same flavour (*ddd*, *uuu* and *sss* respectively), which was in conflict with the Pauli principle. One quark can carry one of the three colors (usually called *red*, *green* and *blue*) and antiquark one of the three anti-colors respectively. Only color-neutral (or white) particles could exist, mesons are assumed to be a color-anticolor pair, while baryons are *red-green-blue* triplets. Gluons also are color-charged and there are 8 types of gluons. Therefore they can interact with themselves [3].

[1] The LHCb experiment at CERN in Geneva confirmed recently existence of $Z(4430)$ - a particle consisting of four quarks [2].

1.2.2 Quantum Chromodynamics potential

As a result of that gluons are massless, one can expect, that the static potential in the QCD will have the similar form like one in the electrodynamics e.g. $\sim 1/r$. In reality the QCD potential is assumed to have the form of [3]

$$V_s = -\frac{4}{3}\frac{\alpha_s}{r} + kr \ , \tag{1.1}$$

where the α_s is a coupling constant of the strong force and the kr part is related with the *confinement*. In comparison to the electromagnetic force, a value of the strong coupling constant is $\alpha_s \approx 1$ and the electromagnetic one is $\alpha = 1/137$.

The fact that quarks does not exist separately, but they are always bound, is called a confinement. As two quarks are pulled apart, the linear part kr in the eq. 1.1 becomes dominant and the potential becomes proportional to the distance. This situation resembles stretching of a string. At some point, when the string is so large it is energetically favourable to create a quark-antiquark pair. At this moment such pair (or pairs) is formed, the string breaks and the confinement is preserved (Fig. 1.2).

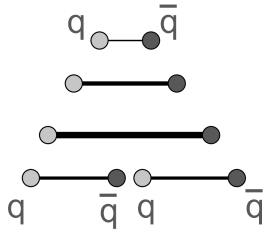

Figure 1.2: A string break and a creation of a pair quark-anti-quark [4].

On the other hand, for the small r, an interaction between the quarks and gluons is dominated by the Coulomb-like term $-\frac{4}{3}\frac{\alpha_s}{r}$. The coupling constant α_s depends on the four-momentum Q^2 transferred in the interation. This dependence is presented in Fig. 1.3. The value α_s decreases with increasing momentum transfer and the interaction becomes weak for large Q^2 ($\alpha_s(Q) \to 0$). Because of weakening of coupling constant, quarks at large energies (or small distances) are starting to behave like free particles. This phenomenon is known as an *asymptotic freedom*. The QCD potential has also temperature dependence - the force strength "melts" with the temperature increase. Therefore the asymptotic freedom is expected to appear in either the case of high baryon densities (small distances between quarks) or very high temperatures. This temperature dependence is illustrated in the Fig. 1.4.

If the coupling constant α_s is small, one can use perturbative methods to calculate physical observables. Perturbative QCD (pQCD) successfully describes hard processes (with large Q^2), such as jet production in high energy proton-antiproton collisions. The applicability of pQCD is defined by the *scale parameter*

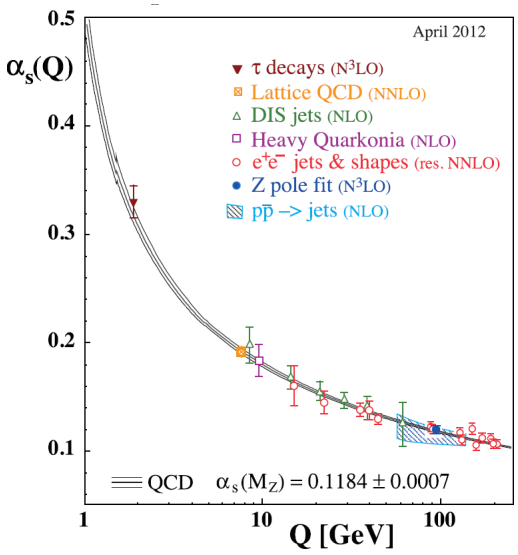

Figure 1.3: Alpha. [5].

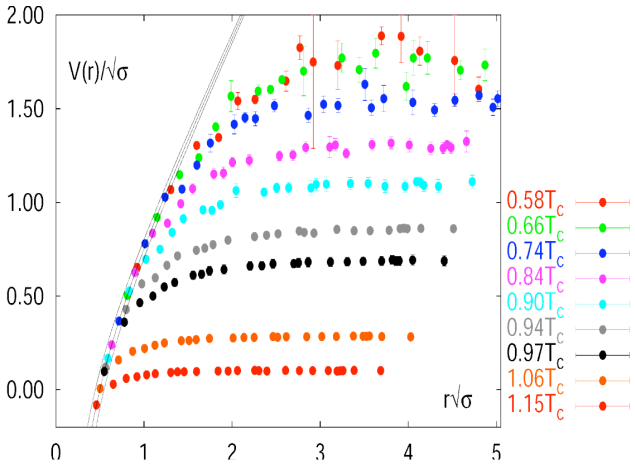

Figure 1.4: The QCD potential for a pair quark-antiquark as a function of distance for different temperatures. [4].

$\Lambda_{QCD} \approx 200$ MeV. If $Q \gg \Lambda_{QCD}$ then the process is in the perturbative domain and can be described by pQCD. A description of soft processes (when $Q < 1$ GeV) is a problem in QCD - perturbative theory breaks down at this scale. Therefore, to describe processes with low Q^2, one has to use alternative methods like Lattice QCD. Lattice QCD (LQCD) is non-perturbative implementation of field theory in which QCD quantities are calculated on a discrete space-time grid. LQCD allows to obtain properties of matter in equilibrium, but there are some limitations. Lattice QCD requires fine lattice spacing to obtain precise results - therefore large

computational resources are necessary. With the constant growth of computing power this problem will become less important. The second problem is that lattice simulations are possible only for baryon density $\mu_B = 0$. At $\mu_B \neq 0$, Lattice QCD breaks down because of the sign problem [6].

1.2.3 The quark-gluon plasma

The new state of matter in which quarks are no longer confined is known as a *quark-gluon plasma* (QGP). The predictions coming from the discrete space-time Lattice QCD calculations reveal a phase transition from the hadronic matter to the quark-gluon plasma at the high temperatures and baryon densities. The results

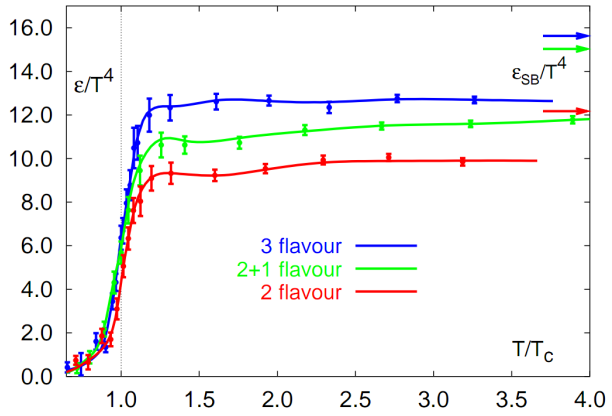

Figure 1.5: A number of degrees of freedom as a function of a temperature [7].

obtained from such calculations are show on Fig. 1.5. The energy density ϵ which is divided by T^4 is a measure of number of degrees of freedom in the system. One can observe significant rise of this value, when the temperature increases past the critical value T_C. Such increase is signaling a phase transition - the formation of QGP [8]. The values of the energy densities plotted in Fig. 1.5 do not reach the Stefan-Boltzmann limit ϵ_{SB} (marked with arrows), which corresponds to the ideal gas. This can indicate some residual interactions in the system. According to the results from the RHIC[2], the new phase of matter behaves more like an ideal fluid, than like a gas [9].

One of the key questions, to which current heavy ion physics tries to find an answer is the value of a critical temperature T_C as a function of a baryon chemical potential μ_B (baryon density), where the phase transition occur. The results coming from the Lattice QCD are presented in the Fig. 1.6. The phase of matter in which quarks and gluons are deconfined is expected to exist at large temperatures. In the region of small temperatures and high baryon densities, a

[2]Relativistic Heavy Ion Collider at Brookhaven National Laboratory in Upton, New York

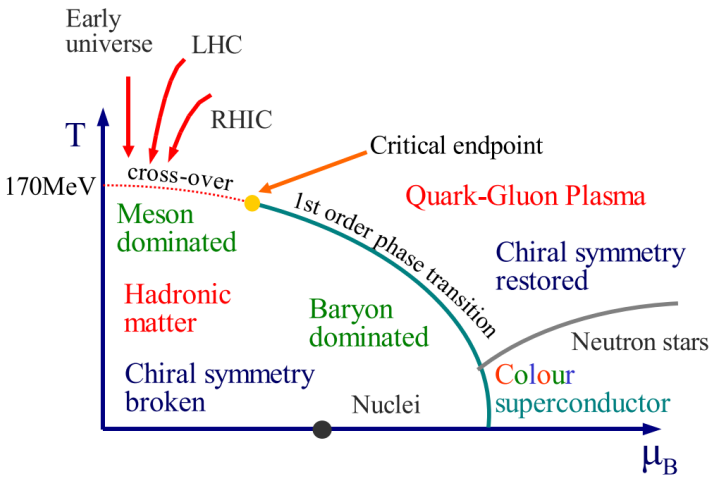

Figure 1.6: Phase diagram coming from the Lattice QCD calculations [8].

different state is supposed to appear - a *colour superconductor*. The phase transition between hadronic matter and QGP is thought to be of 1st order at $\mu_B \gg 0$. However as $\mu_B \to 0$ quarks' masses become significant and a sharp transition transforms into a rapid but smooth cross-over. It is believed that in Pb-Pb collisions observed at the LHC[3], the created matter has high enough temperature to be in the quark-gluon plasma phase, then cools down and converts into hadrons, undergoing a smooth transition [8].

1.3 Relativistic heavy ion collisions

[3]Large Hadron Collider at CERN, Geneva

Chapter 2

Therminator model

THERMINATOR [10] is a Monte Carlo event generator designed to investigate the particle production in the relativistic heavy ion collisions. The functionality of the code includes a generation of the stable particles and unstable resonances at the chosen hypersurface model. It performs the statistical hadronization which is followed by space-time evolution of particles and the decay of resonances. The key element of this method is an inclusion of a complete list of hadronic resonances, which contribute very significantly to the observables. The second version of THERMINATOR [11] comes with a posibility to incorporate any shape of freeze-out hypersurface and the expansion velocity field, especially those generated externally with various hydrodynamic codes.

2.1 (3+1)-dimensional viscous hydrodynamics

Most of the relativistic viscous hydrodynamic calculations are done in (2+1)-dimensions. Such simplification assumes boost-invariance of a matter created in a collision. Experimental data reveals that no boost-invariant region is formed in the collisions [12]. Hence, for the better description of created system a (3+1)-dimensional model is required.

In the four dimensional relativistic dynamics one can describe a system using a space-time four-vector $x^\nu = (ct, x, y, z)$, a velocity four-vector $u^\nu = \gamma(c, v_x, v_y, v_z)$ and a energy-momentum tensor $T^{\mu\nu}$. The particular components of $T^{\mu\nu}$ have a following meaning:

- T^{00} - an energy density,
- $cT^{0\alpha}$ - an energy flux across a surface x^α,
- $T^{\alpha 0}$ - an α-momentum flux across a surface x^α multiplied by c,
- $T^{\alpha\beta}$ - components of momentum flux density tensor,

where $\gamma = (1 - v^2/c^2)^{-1/2}$ is Lorentz factor and $\alpha, \beta \in \{1, 2, 3\}$. Using u^ν one can express $T^{\mu\nu}$ as follows [13]:

$$T_0^{\mu\nu} = (e + p)u^\mu u^\nu - pg^{\mu\nu} \tag{2.1}$$

where e is an energy density, p is a pressure and $g^{\mu\nu}$ is an inverse metric tensor:

$$g^{\mu\nu} = \begin{bmatrix} 1 & 0 & 0 & 0 \\ 0 & -1 & 0 & 0 \\ 0 & 0 & -1 & 0 \\ 0 & 0 & 0 & -1 \end{bmatrix}. \tag{2.2}$$

The presented version of energy-momentum tensor (2.1) can be used to describe dynamics of a perfect fluid. To take into account influence of viscosity, one has to apply the following corrections coming from shear $\pi^{\mu\nu}$ and bulk Π viscosities [14]:

$$T^{\mu\nu} = T_0^{\mu\nu} + \pi^{\mu\nu} + \Pi(g^{\mu\nu} - u^\mu u^\nu). \tag{2.3}$$

The stress tensor $\pi^{\mu\nu}$ and the bulk viscosity Π are solutions of dynamical equations in the second order viscous hydrodynamic framework [13]. The comparison of hydrodynamics calculations with the experimental results reveal, that the shear viscosity divided by entropy η/s has to be small and close to the AdS/CFT estimate η/s = 0.08 [14, 15].

When using $T^{\mu\nu}$ to describe system evolving close to local thermodynamic equilibrium, relativistic hydrodynamic equations in a form of:

$$\partial_\mu T^{\mu\nu} = 0 \tag{2.4}$$

can be used to describe the dynamics of the local energy density, pressure and flow velocity.

Hydrodynamic calculations are starting from the Glauber [1] model initial conditions. The collective expansion of a fluid ends at the freeze-out hypersurface. That surface is usually defined as a constant temperature surface, or equivalently as a cut-off in local energy density. The freeze-out is assumed to occur at the temperature T = 140 MeV.

2.2 Statistical hadronization

Statistical description of heavy ion collision has been successfully used to describe quantitatively *soft* physics, i.e. the regime with the transverse momentum not exceeding 2 GeV. The basic assumption of the statistical approach of evolution of the quark-gluon plasma is that at some point of the space-time evolution of the fireball, the thermal equilibrium is reached. When

[1] The Glauber Model is used to calculate "geometrical" parameters of a collision like an impact parameter, number of participating nucleons or number of binary collisions.

the system is in the thermal equilibrium the local phase-space densities of particles follow the Fermi-Dirac or Bose-Einstein statistical distributions. At the end of the plasma expansion, the freeze-out occurs. The freeze-out model incorporated in the THERMINATOR model assumes, that chemical and thermal freeze-out occur at the same time.

2.2.1 Cooper-Frye formalism

The result of the hydrodynamic calculations is the freeze-out hypersurface Σ^μ. A three-dimensional element of the surface is defined as [11]

$$d\Sigma_\mu = \epsilon_{\mu\alpha\beta\gamma} \frac{\partial x^\alpha}{\partial \alpha} \frac{\partial x^\beta}{\partial \beta} \frac{\partial x^\gamma}{\partial \gamma} d\alpha d\beta d\gamma, \tag{2.5}$$

where $\epsilon_{\mu\alpha\beta\gamma}$ is the Levi-Civita tensor and the variables $\alpha, \beta, \gamma \in \{1, 2, 3\}$ are used to parametrize the three-dimensional freeze-out hypersurface in the Minkowski four-dimensional space. The Levi-Civita tensor is equal to 1 when the indices form an even permutation (eg. ϵ_{0123}), to -1 when the permutation is odd (e.g. ϵ_{2134}) and has a value of 0 if any index is repeated. Therefore [11],

$$d\Sigma_0 = \begin{vmatrix} \frac{\partial x}{\partial \alpha} & \frac{\partial x}{\partial \beta} & \frac{\partial x}{\partial \gamma} \\ \frac{\partial y}{\partial \alpha} & \frac{\partial y}{\partial \beta} & \frac{\partial y}{\partial \gamma} \\ \frac{\partial z}{\partial \alpha} & \frac{\partial z}{\partial \beta} & \frac{\partial z}{\partial \gamma} \end{vmatrix} d\alpha d\beta d\gamma \tag{2.6}$$

and the remaining components are obtained by cyclic permutations of t, x, y and z.

One can obtain the number of hadrons produced on the hypersurface Σ^μ from the Cooper-Frye formalism. The following integral yields the total number of created particles [11]:

$$N = (2s+1) \int \frac{d^3p}{(2\pi)^3 E_p} \int d\Sigma_\mu(x) p^\mu f(x,p), \tag{2.7}$$

where

$$f(p \cdot u) = \left\{ ex \left[\frac{p_\mu u^\mu - (B\mu_B + I_3\mu_{I_3} + S\mu_S + C\mu_C)}{T} \right] \pm 1 \right\}^{-1} \tag{2.8}$$

is the phase-space distribution for particles (for stable ones and resonances). For the Fermi-Dirac distribution in the 2.8 there is a plus sign and for Bose-Einstein statistics minus sign respectively. The thermodynamic quantities appearing in the $f(\cdot)$ are T - temperature, μ_B - baryon chemical potential, μ_{I_3} - isospin chemical potential, μ_S - strange chemical potential, μ_C - charmed chemical potential and the s is a spin of a particle. One can simply derive from equation 2.7, the dependence of the momentum density [16]:

$$E\frac{dN}{d^3p} = \int f(x,p) p^\mu d\Sigma_\mu. \tag{2.9}$$

The equations presented above are directly used in the THERMINATOR to generate the hadrons with the Monte-Carlo method.

Chapter 3

Particle interferometry

3.1 HBT interferometry

3.2 Intensity interferometry in heavy ion collisions

3.2.1 Theoretical approach

Two particle wave function

Source function

Theoretical correlation function

Spherical harmonics decomposition of correlation function

3.2.2 Experimental approach

3.3 Scaling of femtoscopic radii

Chapter 4

Results

4.1 Identical particles correlations

4.2 Results of the fit

4.3 Discussion of results

Chapter 5

Summary

Bibliography

[1] Standard Model of Elementary Paticles - Wikipedia, the free encyclopedia `http://en.wikipedia.org/wiki/standard_model`.

[2] R. Aaij et al. (LHCb Collaboration). Observation of the resonant character of the $z(4430)^-$ state. *Phys. Rev. Lett.*, 112:222002, Jun 2014.

[3] Donald H. Perkins. *Introduction to High Energy Physics*. Cambridge University Press, fourth edition, 2000. Cambridge Books Online.

[4] G. Odyniec. *Phase Diagram of Quantum Chromo-Dynamics* - course at Faculty of Physics, Warsaw University of Technology, Jun 2012.

[5] J. Beringer et al. (Particle Data Group). The Review of Particle Physics. *Phys. Rev.*, D86:010001, 2012.

[6] Z. Fodor and S.D. Katz. The Phase diagram of quantum chromodynamics. 2009.

[7] F. Karsch. Lattice results on QCD thermodynamics. *Nuclear Physics A*, 698(1-4):199 – 208, 2002.

[8] Adam Kisiel. *Studies of non-identical meson-meson correlations at low relative velocities in relativistic heavy-ion collisions registered in the STAR experiment*. PhD thesis, Warsaw University of Technology, Aug 2004.

[9] J. Bartke. *Relativistic Heavy Ion Physics*. World Scientific Pub., 2009.

[10] Adam Kisiel, Tomasz Taluc, Wojciech Broniowski, and Wojciech Florkowski. THERMINATOR: THERMal heavy-IoN generATOR. *Comput.Phys.Commun.*, 174:669–687, 2006.

[11] Mikolaj Chojnacki, Adam Kisiel, Wojciech Florkowski, and Wojciech Broniowski. THERMINATOR 2: THERMal heavy IoN generATOR 2. *Comput.Phys.Commun.*, 183:746–773, 2012.

[12] I. et al (BRAHMS Collaboration) Bearden. Charged meson rapidity distributions in central $\mathrm{Au} + \mathrm{Au}$ collisions at $\sqrt{s_{NN}} = 200\ \mathrm{GeV}$. *Phys. Rev. Lett.*, 94:162301, Apr 2005.

[13] W. Israel and J.M. Stewart. Transient relativistic thermodynamics and kinetic theory. *Annals of Physics*, 118(2):341 – 372, 1979.

[14] Piotr Bożek. Flow and interferometry in (3 + 1)-dimensional viscous hydrodynamics. *Phys. Rev. C*, 85:034901, Mar 2012.

[15] K. Kovtun, P. D. T. Son, and A. O. Starinets. Viscosity in strongly interacting quantum field theories from black hole physics. *Phys. Rev. Lett.*, 94:111601, Mar 2005.

[16] Fred Cooper and Graham Frye. Single-particle distribution in the hydrodynamic and statistical thermodynamic models of multiparticle production. *Phys. Rev. D*, 10:186–189, Jul 1974.

List of Figures